THE BALTIC JOURNAL
OF ROAD AND BRIDGE ENGINEERING

ISSN 1822-427X / eISSN 1822-4288
2015 Volume 10(2): 118–125

A COMBINED CONTROL STRATEGY FOR VIBRATION MITIGATIONS OF A SUSPENSION BRIDGE INDUCED BY VEHICLE BRAKING FORCE

Meng-Gang Yang[1]✉, Chun-Sheng Cai[2], Biao Wei[3]

[1, 3]*School of Civil Engineering, Central South University, No. 68 Shaoshan South Road, Changsha 410075, PR China*
[2]*Dept of Civil and Environmental Engineering, Louisiana State University, Baton Rouge, LA 70803, USA*
E-mails: [1]*mgyang@csu.edu.cn;* [2]*cscai@lsu.edu;* [3]*weibiaocsu@163.com*

Abstract. In order to mitigate the excessive longitudinal displacement responses of suspension bridge girders induced by vehicle braking force, as one of the possible dynamic loadings, a combined control strategy consisting of viscous dampers and friction pendulum bearings is developed in this paper. Firstly, the vehicle composition and the braking force models of the Pingsheng Bridge are obtained by traffic survey and testing results, respectively. Then, the vibration response analysis for the bridge under the braking force is implemented using the MIDAS finite element model. Furthermore, viscous dampers and friction pendulum bearings are separately employed to reduce the vibration responses. The influence matrix method is first used to determine the optimal parameters of viscous dampers. Finally, the effect of the combined control strategy for the vibration control is investigated. The numerical analysis results indicate that utilizing the influence matrix method for the parameter optimization of viscous dampers is feasible and effective. It is also shown that the longitudinal displacement response of the Pingsheng Bridge subjected to the vehicle braking force can be effectively mitigated by viscous dampers, friction pendulum bearings or the combined control with the optimized parameters, and the combined control outperforms the viscous dampers or the friction pendulum bearings alone.

Keywords: suspension bridge, vehicle braking force, viscous damper, friction pendulum bearing, combined control, vibration mitigation.

1. Introduction

Suspension bridges are widely employed in long-span bridges since their internal force can be controlled well owing to the good energy-dissipating performance decided by its long period of the first-order longitudinal floating mode. However, the longitudinal displacement of the girders induced by vehicle braking forces, as one of the possible dynamic loadings, may be excessive based on the following factors:

The number of vehicles running on a wide and long-span bridge is large. Pingsheng Bridge, as a case study in this paper, has a 350 m main span and twin decks, each of which carries a five-lane highway and is 19.70 m in width. Dynamic analysis for the Pingsheng Bridge induced by the vehicle braking force needs to be investigated.

For the separate twin-deck bridge, each deck serves one-way lane, so the braking forces of all the vehicles in each deck have the same direction. The accumulative vehicle braking force may be large enough to cause the longitudinal vibration of the deck.

Vehicle braking time after being driven at a high speed is longer than at a low speed. Although the braking force is generally small compared with the bridge mass, the dynamics response may still be excessive because of the longer braking time.

The excessive longitudinal displacements cause many problems such as bridge bearing damage, destruction of expansion joints, fatigue fracture of short hanger cables, pounding between the girders and adjacent approach bridges and so on. These problems certainly result in considerable difficulties in bridge maintenance, and even affect their normal operation. Therefore, it is very necessary to restrain the excessive longitudinal displacements.

Some researches on seismic response control of the girder displacements for suspension bridges were investigated (Apaydin 2010; Yang *et al.* 2011, 2013), but the studies on the longitudinal displacement mitigation of bridge girders subjected to braking force are quite few. Liu *et al.* (2010) and Qu *et al.* (2009) presented longitudinal vibration response controls for a floating-type cable-stayed bridge induced by train braking forces.

Viscous dampers are commonly used for vibration control in civil engineering since it has the excellent characteristics with damping energy dissipation, does not increase the stiffness of the structure, and does not restrain

Copyright © 2015 Vilnius Gediminas Technical University (VGTU) Press Technika
doi:10.3846/bjrbe.2015.15

the temperature deformation. Seismic protection and retrofit of building structures can be achieved by viscous dampers (Hart *et al.* 2010; Hwang *et al.* 2007; Krishnamoorthy 2011). Martinez-Rodrigo *et al.* (2010) presented the application of viscous dampers to mitigate the excessive resonant responses of railway bridges under high-speed moving loads, and Hwang and Tseng (2005) and Cheng *et al.* (2010) presented the vibration control techniques of viscous dampers for highway bridges and bridge cables. In addition, viscous dampers were investigated by Wang *et al.* (2005) to suppress the wind-induced vibrations of high-rise buildings and bridge cables. In these previous researches, the design parameters of viscous dampers were determined by the method of trial and error. As a result, the calculating procedure is complicated and the obtained parameters are not necessarily optimal. In this paper, a new application domain of viscous dampers for the vibration control under vehicle braking forces is developed, and the influence matrix method is first applied for the parameter optimization of viscous dampers.

Friction pendulum bearings (FPBs) belong to an effective friction-sliding isolated system, and have self-return advantage. Vibration responses of the structure with FPBs can be mitigated since the vibration period is prolonged and the excitation energy is dissipated by the sliding friction. At present, the FPB is mainly applied for seismic response control of buildings and bridges (Ates *et al.* 2006; Jangid 2008; Panchal *et al.* 2009). A new attempt that the FPB is used to reduce the vibration response of a suspension bridge subjected to vehicle braking forces will be investigated in this paper.

If the longitudinal displacements of the girders still exceed the limited value of the bridge bearings and the allowable value of the expansion joint when viscous dampers and FPBs are separately used, a combined control strategy consisting of both viscous dampers and FPBs can be considered.

The present study aims at developing a combined control strategy for vibration mitigations of a suspension bridge induced by vehicle braking forces. Firstly, the vehicle braking force models for the Pingsheng Bridge are obtained by traffic survey and testing results. Then, the MIDAS 3-D dynamic finite element model for the bridge is established, and the vibration response analysis is completed under the braking force. Finally, the combined control strategy consisting of both viscous dampers and FPBs is developed to reduce the vibration responses in which the influence matrix method is first applied for the parameter optimization of viscous dampers, and the effectiveness of vibration mitigations is verified by numerical analysis.

2. Vehicle braking force acting on Pingsheng Bridge

2.1. Pingsheng Bridge

The Pingsheng Bridge is a self-anchored suspension bridge with a single tower in the Foshan city of Guangdong province, China. The general layout of the bridge is given in Fig. 1. The bridge has a main span of 350 m and is ranked the first among its kind. The tower of the bridge is made of concrete and is 143.38 m in height. The sag-to-span ratio for the steel main cables is 1/12.5 in the main span. The bridge has twin decks to carry a ten-lane highway, and each deck is 19.70 m in width and has five lanes. The girder of the main span is made of structural steel and that of the side span is made of concrete. The design vehicle speed is 80 km/h. Table 1 lists the main structural design parameters of the Pingsheng Bridge.

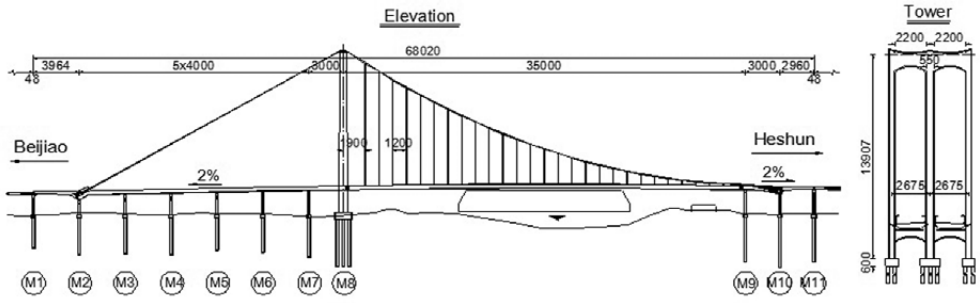

Fig. 1. General layout of Pingsheng bridge, cm

Table 1. Main structural design parameters of the Pingsheng Bridge

Member	E, kN/m^2	A, m^2	I_s, m^4	I_t, m^4	I_p, m^4
Steel girder	$2.1 \cdot 10^8$	1.289	48.133	2.804	6.198
Concrete girder	$3.5 \cdot 10^7$	18.368	794.948	32.416	99.092
Tower	$3.5 \cdot 10^7$	15.507	83.673	41.024	81.143
Cable	$1.9 \cdot 10^8$	0.1245	0	0	0
Suspender	$1.9 \cdot 10^8$	0.00298	0	0	0
Pier	$3.0 \cdot 10^7$	5.600	3.659	1.867	4.197

2.2. Vehicle composition of Pingsheng Bridge

The vehicle types and their proportions in transportation are the two main factors in vehicle composition. Since different road has different vehicle composition, the vehicle composition for a specific road should be obtained by traffic survey. It had been investigated by traffic management department that there were eight types of vehicles on the Guangfo highway linking Guangzhou city to Foshan city in China, as listed in Table 2. Since the Pingsheng Bridge is a connection between an urban road in the Foshan city and the Guangfo express highway, these data can be used in its dynamic analysis.

According to Table 2, small passenger cars have a high proportion in the vehicle composition, followed by medium-sized vehicles, large cars and towed vehicles. On the whole, this vehicle composition of the Guangfo highway is similar with that of other highways in China. In fact, some types of vehicles including minivan, passenger-cargo dual-purpose cars, minicars and light cars, have similar characteristics with small passenger cars in the number of axles and self-weight, and their proportions in the vehicle composition are low. Therefore, minivans, passenger-cargo dual-purpose cars, minicars, light cars, and small passenger cars can be gathered and classified into light vehicles. Finally, the vehicle composition of the Pingsheng Bridge in this paper is simplified into four types, including light vehicles, medium-sized vehicles, large cars, and heavy vehicles. Their proportions in the vehicle composition are listed in Table 3. However, the proportion of the heavy vehicle is increasing according to the investigation of Cantero *et al.* (2011), which will make the response induced by vehicle braking force larger.

2.3. Braking force model

The vehicle braking process includes four phases: (1) the response time of the brake system, about 0.015~0.03 s for a hydraulic brake system and 0.05~0.06 s for a air brake system, respectively; (2) the action time of the brake, 0.15~0.3 s for a hydraulic brake system and 0.3~0.8 s for an air brake system, respectively, and the braking force gradually increases in this stage; (3) the continuous brake time, and the braking force is relatively stable in this stage; (4) the loose time of

Table 2. Taffic survey on Guangfo highway

No.	Vehicle type	Number of axles	Proportion	Note
1	Minivan	2	2.5	
2	Passenger-cargo dual-purpose car	2	3.5	
3	Minicar	2	3.3	
4	Small passenger car	2	52.6	
5	Light car	2	3.9	Carrying capacity: <2 t Seating capacity: <11
6	Medium-sized vehicle	2~3	14.9	Carrying capacity: 2 t ~7 t Seating capacity: 11~25
7	Large car	2~4	12.2	Carrying capacity: 7 t ~14 t Seating capacity: >25
8	Towed vehicle	4~5	7.1	Carrying capacity: >14 t

Table 3. Vehicle composition of the Pingsheng Bridge

Vehicle type	Note	Proportion, %
Light vehicle	Including microvan, passenger-cargo dual-purpose car, minicar, small passenger car and light car	65.8
Medium-sized vehicle	Definition see Table 2	14.9
Large car	Definition see Table 2	12.2
Heavy vehicle	i.e. towed vehicle	7.1

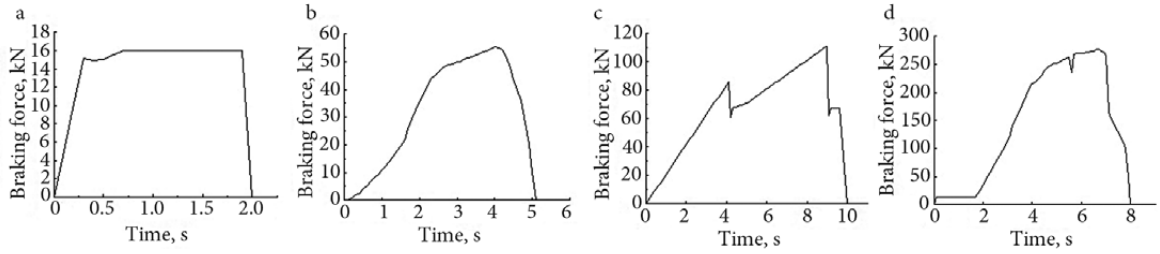

Fig. 2. Vehicle braking force model: a –light vehicle; b – medium-sized vehicle; c – large car; d – heavy vehicle

the brake system. The brake pedal is released by the driver in this stage and the braking process is over after this stage.

To obtain the braking force models, firstly the average gross weights of the four types of vehicles are obtained from the statistical analysis by traffic management department. Then, the braking force test for them with the average gross weights was conducted at the velocity of 50 km/h by Peng and Wang (2003). Finally, according to the testing results and theoretical analysis, the complete vehicle braking ratios of the braking force to the vehicle gross weight and the braking force models are obtained. The vehicle braking force models are shown in Fig. 2.

3. Vibration response analysis

3.1. Finite element model

The dynamic 3-D MIADS finite element model of the Pingsheng Bridge is constructed and shown in Fig. 3. In this model, the bridge is discretized into 716 elements, including 448 beam elements, 108 truss elements and 160 cable elements. The girder, tower and pier are modeled with spatial beam elements; the suspender is modeled with spatial truss elements; and the cable is modeled with two-node spatial catenary cable elements proposed by Yang *et al.* (2010). In the vibration response analysis, the effect of geometrical non-linearity under dead loads can be incorporated by geometric stiffness matrixes of these elements. It has been known via static analysis that the foundations supporting the tower and the piers are quite stiff. Thus, the foundation deformations are not included in this model and the degrees of freedom associated with these nodes at the bottom of the tower and the piers are restrained.

3.2. Vehicle number for dynamic analysis

The total vehicle braking force acting on the Pingsheng Bridge is determined by the number and the braking force models of the vehicles. The braking force models have been discussed earlier. The vehicle number is related to the length of the bridge span, the lane number and the velocity, besides the vehicle composition. Although the design vehicle speed is 80 km/h, the practical average velocity is about 50 km/h for urban road. The vehicle space is about 20 m based on the relationship between the car-following safe distance and the velocity investigated by Hoseini *et al.* (2009), which is essentially coincident with the data by an actual survey. Therefore, each lane can run 27 vehicles within the length of the bridge span, including 18 light vehicles, 4 medium-sized vehicles, 3 large cars, and 2 heavy vehicles according to the vehicle composition. The reduction factor is 0.6 for five lanes of one deck by the Chinese code. Thus, the lane number after reduction is 3.0. Therefore, there are totally 81 vehicles on the bridge for dynamic analysis, including 54 light vehicles, 12 medium-sized vehicles, 9 large cars and 6 heavy vehicles.

3.3. Longitudinal displacement response

The longitudinal displacement response of the Pingsheng Bridge subjected to the braking force of 81 vehicles is gained by finite element analysis (the uncontrolled curve in Fig. 4). The peak value of the longitudinal displacement of the girder reaches 37.7 cm, exceeding the limited value of 25 cm of the bridge bearings and the allowable value of 22 cm of the expansion joints excluding the displacement value under the action of the concrete shrinkage and creep, temperature and live load, which may lead to the destruction of the bearings and the expansion joints. Therefore, the excess longitudinal displacements of the girders subjected to vehicle braking forces should be necessarily controlled.

4. Viscous damper for vibration mitigation

4.1. Mechanical model for viscous damper

The damper force of viscous dampers can be expressed as:

$$F = Cv^{\alpha}, \tag{1}$$

where F – the damping force, kN; C – the viscous damping coefficient, kN·s/m; v – the relative velocity of the damper, m/s; α – the velocity exponent.

It is known from Eq (1) that the damping force is decided by the two parameters: the viscous damping coefficient C and the velocity exponent α. The damping force has a linear relationship with the viscous damping coefficient, yet is non-linear to the velocity exponent. In the application of civil engineering, C is usually in the range of 1000~10 000 kN·s/m, and α is in the range of 0.2~1.0.

4.2. Influence matrix method used in this study

The influence matrix method is an efficient and simple structural optimization method. To reduce the displacement response of the girders subjected to vehicle braking force, two viscous dampers are supposed to be installed in the longitudinal direction between the tower and the girder of the Pingsheng Bridge. According to Eq (1), the effect of vibration mitigation is determined by the two parameters: C and α. In this study, the influence matrix method is applied to obtain the reasonable optimal design parameters C and α of the dampers. The formula is as below:

$$[A]\mathbf{X} = \mathbf{D}, \tag{2}$$

where $[A]$ – the influence matrix; $\mathbf{X}$ and $\mathbf{D}$ – the passively controlled vector and the actively controlled vector, respectively.

The weight matrix [ρ] is used to consider the importance of different actively controlled element in the vector $\mathbf{D}$, so Eq (2) can be re-written as following:

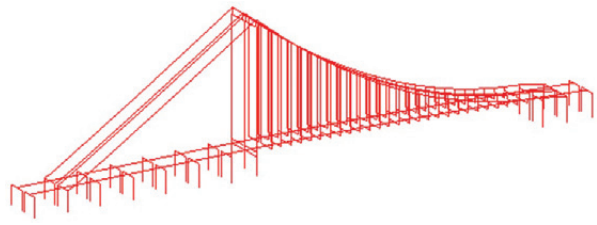

Fig. 3. 3-D finite element model of the Pingsheng Bridge

$$[\rho][A]\mathbf{X}=[\rho]\mathbf{D}. \quad (3)$$

In this study, the passively controlled elements in the vector **X** are the parameters C and α, and the actively controlled vector **D** is the control objective (i.e. the reduction rate of key displacement or internal force). For the Pingsheng Bridge, the longitudinal displacement of the girder, the moment and the shear force at the bottom of the tower are the most important elements which need to be controlled subjected to vehicle braking forces. Therefore, the vectors **X** and **D** can be expressed as:

$$\mathbf{X}=\begin{Bmatrix} C \\ \alpha \end{Bmatrix}, \mathbf{D}=\begin{Bmatrix} S \\ M \\ Q \end{Bmatrix}, \quad (4)$$

where C and α – the parameters of the viscous damper; S, M and Q – the reduction rates of the longitudinal displacement of the girder, the moment, and the shear force at the bottom of the tower, respectively.

Since the element number in the passively controlled vector **X** is not equal to that in the actively controlled vector **D**, the least square method is used to solve Eq (3). One can obtain:

$$[A]^T[\rho]^2[A]\mathbf{X}=[A]^T[\rho]^2\mathbf{D}. \quad (5)$$

Therefore, the vector **X** can be solved from Eq (5)

$$\mathbf{X}=\left([A]^T[\rho]^2[A]\right)^{-1}[A]^T[\rho]^2\mathbf{D}. \quad (6)$$

4.3. Parameter optimization

By finite element analysis for the Pingsheng Bridge with two viscous dampers, the influence matrix $[A]$ is obtained as following:

$$[A]=\begin{bmatrix} -0.0122 & 0.127 \\ -9165 & 93130 \\ -55.3 & 494.4 \end{bmatrix}. \quad (7)$$

Considering that the mitigation of the longitudinal displacement of the girders is more important than that of the internal force for the Pingsheng Bridge, the weight matrix [ρ] and the actively controlled vector **D** are set as:

$$[\rho]=\begin{bmatrix} 0.8 & 0 & 0 \\ 0 & 0.15 & 0 \\ 0 & 0 & 0.05 \end{bmatrix}, \mathbf{D}=\begin{Bmatrix} 35\% \\ 15\% \\ 10\% \end{Bmatrix}. \quad (8)$$

In the vector **D**, every element in the vector is the response reduction rate β, which is defined as

$$\beta=\frac{e_0-e_1}{e_0}\cdot 100\%, \quad (9)$$

where e_0 and e_1 – the uncontrolled and controlled response, respectively.

Substituting Eqs (7)–(8) into Eq (6), the optimal parameters C and α of the dampers can be determined as 2640 kN·s/m and 0.5, respectively.

Evidently, the influence matrix $[A]$ is of vital importance in determining the optimal parameters of the dampers. Therefore, it must have a good stability. In theory, the influence matrix method is only suitable for linear system. Actually, high non-linearity of suspension bridges mainly occurs in the construction process, while the non-linearity is not obvious during the service stage, and its influence on seismic response for the bridge is less than 6% by the investigation of the first author. On the other hand, the non-linearity of the damper has little influence on the matrix $[A]$ when the values of the parameters are in the range given in section 4.1. Therefore, the influence matrix method is feasible to be used for parameter optimizations of viscous dampers that are applied in vibration mitigations of the bridge subjected to vehicle braking forces.

4.4. Effect of vibration mitigation

On the basis of the optimal parameters C = 2640 kN·s/m and α = 0.5, the dynamic responses of the Pingsheng Bridge with viscous dampers subjected to vehicle braking forces are calculated. The results show that viscous dampers with optimal parameters not only reduce the longitudinal displacement obviously, but also decrease the internal forces at the bottom of the tower. Fig. 4 gives the comparison of the longitudinal displacement of the girders between the floating system (uncontrolled) and damped system (viscous damper). The maximum moment and shear force at the bottom of the tower are seen in Table 4. The peak value of the displacement, the maximum moment, and the maximum shear force decrease by 34.54%, 15.9% and 12.4%, respectively. In addition, the reduction rates obtained by finite element analysis are close to the objective reduction rates in Eq (8), indicating that the influence matrix method is effective to determine the optimal parameters of viscous dampers for vibration mitigations. The peak value of the displacement with viscous dampers is 24.68 cm that still exceeds the allowable value of 22 cm of the expansion joints.

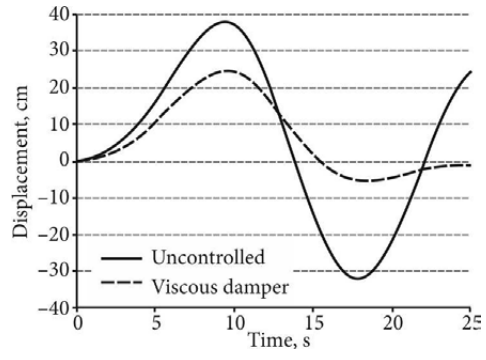

Fig. 4. Vibration reduction effect by viscous damper

5. Friction pendulum bearing (FPB) for vibration mitigation

5.1. FPB mechanical model

The damping force of FPBs is composed of the restoring force and the friction force, and can be expressed as:

$$F = \frac{W}{R}x + \mu W \operatorname{sgn}(\dot{x}), \tag{10}$$

where W – the vertical reaction force, kN; R – the curvature radius of sliding surface, m; μ – the friction coefficient; x – the displacement, m; $\dot{x}$ – the velocity, m/s; sgn(·) – the signum function.

The mechanical model has a non-linear characteritic, and can be simplified into a linear model which contains the equivalent stiffness and the equivalent damping ratio in the finite element analysis. The equivalent stiffness and the equivalent damping ratio are given as:

$$K_{eff} = \frac{W}{R} + \frac{\mu W}{D}, \xi_{eff} = \frac{2}{\pi}\left(\frac{\mu}{\mu + \frac{D}{R}}\right). \tag{11}$$

where K_{eff} – the equivalent stiffness, kN/m; ξ_{eff} – the equivalent damping ratio; D – the design diaplacement of the bearing, m.

It can be seen from Eq (11) that the equivalent linear model is only determined by the two parameters R and m. Therefore, obtaining the optimized parameters is the first step for FPBs to be applied in vibration mitigations.

5.2. Analysis of FPB parameters

The friction coefficient m is related to the material of the interface and the sliding velocity. Teflon is a commonly-used material for the FPB interface, and its friction coefficient is in the range of 0.02~0.12. The stable friction coefficient is in the range of 0.06~0.12 when the sliding velocity exceeds a certain value, and is in the range of 0.02~0.06 when the sliding velocity approaches to 0. Considering that the sliding velocity of the bearing is low under the vehicle braking force, the range of friction coefficient m is chosen as 0.02~0.06.

The upper limit value of the curvature radius of the sliding surface R is determined by the self-return requirement. The FPB cannot return to the original position if the restoring force is smaller than the friction force. Therefore, it is required: $R < \frac{D}{\mu}$. If the design diaplacement D of the bearing is chosen as 25 cm, one has $R < 2.5$ m. On the other hand, the vertical displacement of the sliding surface increases with the decreasing curvature radius. Therefore, the lower limit value of the curvature radius R is determined by the restriction of the vertical displacement of the bearing. It is commonly required: $R \geq 0.5$ m. As such, the reasonable range of the curvature radius is chosen as 0.5~2.0 m.

To obtain the optimum parameters for the preferable performance in vibration mitigations, twenty cases are considered in the finite element analysis. In these cases, the friction coefficient m is set as 0.02, 0.03, 0.04, 0.05, and 0.06, and the curvature radius R is set as 0.5 m, 1.0 m, 1.5 m, and 2.0 m. For every pier of the Pingsheng Bridge, two bearings are supposed to be installed. The maximum displacement of the girder and the maximum moment at the bottom of the tower are shown in Fig. 5. The displacement and the moment increase with the increasing curvature radius R, while decrease with the increasing friction coefficient μ. Therefore, it is obvious that the optimum parameters R and μ are 0.5 m and 0.06, respectively.

5.3. Effect of vibration mitigation

On the basis of the optimum parameters R = 0.5 m and μ = 0.06, the dynamics responses of the Pingsheng Bridge with FPBs induced by the vehicle braking force are calculated. The longitudinal displacement response of the girder is shown in Fig. 6. The peak value of the displacement is 27.06 cm and reduced by 28.22%. Also the maximum moment and the shear force at the bottom of the tower are reduced by 14.6% and 12.5%, respectively (Table 4). Therefore, FPBs with the optimum parameters have good effects

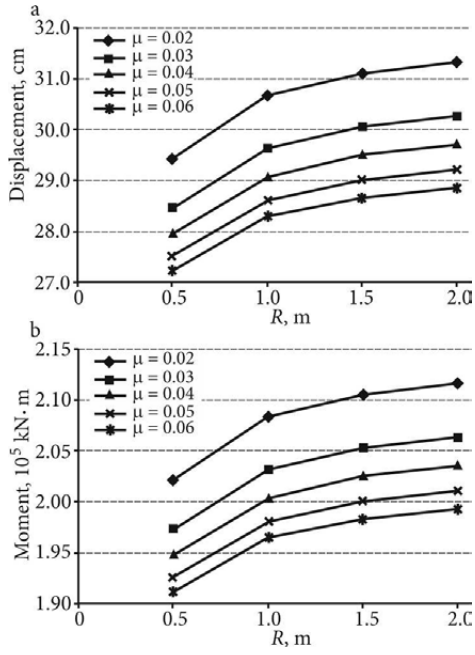

Fig. 5. Variation of the key displacement and moment with R and μ: a – maximum displacement of the girder; b – maximum moment at the bottom of the tower

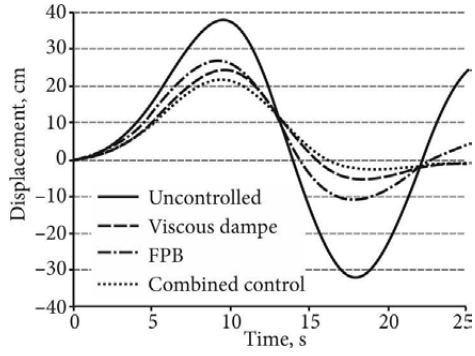

Fig. 6. Vibration reduction effect by different control strategy

Table 4. The maximum moment and shear force at the bottom of the tower

Item		Floating system (Uncontrolled)	Damped system (Controlled)		
			Viscous damper	FPB	Combined
Moment	Value (kN·m)	223 740	188 243	191 099	171 095
	β	–	15.9%	14.6%	23.5%
Shear force	Value (kN)	1674	1466	1464	1349
	β	–	12.4%	12.5%	19.4

of vibration mitigations on suspension bridges. However, the peak value of the displacement with FPBs still exceeds the limited value of 25 cm of the bridge bearings and the allowable value of 22 cm of the expansion joints.

6. Combined control strategy

According to the foregoing investigation, it has been known that viscous dampers and FPBs can both reduce the longitudinal response of the bridge subjected to the vehicle braking force. To meet the need of the limited value of the bridge bearings and the allowable value of the expansion joints, a control strategy combining viscous dampers and FPBs is put forward. In this strategy, the optimal parameters of viscous damper and FPB are adopted (i.e. C = 2640 kN·s/m, α = 0.5, R = 0.5 m and μ = 0.06), and the number and installed position of those are the same as stated above. By finite element analysis, the displacement response of the girder is shown in Fig. 6, and the maximum moment and shear force at the bottom of the tower are given in Table 4. The peak value of the displacement, the maximum moment, and the maximum shear force are reduced by 42.17%, 23.5% and 19.4%, respectively. It has been verified by Fig. 6 and Table 4 that the combined control performs better than an independent application of either viscous dampers or FPBs. The peak value of the displacement with a combined control is 21.8 cm, within the limited value of the bridge bearings and the allowable value of the expansion joints. The combined control strategy can meet the design requirement of the bridge bearings and the expansion joints induced by the vehicle braking force.

7. Conclusions

1. The paper has presented a combined control strategy consisting of viscous dampers and friction pendulum bearings, which has been developed to mitigate the excessive longitudinal displacement response of a suspension bridge induced by vehicle braking forces, as one of the possible dynamic loadings.

2. Based on the vehicle braking force models obtained by testing results and the MIDAS finite element model, the vibration responses are analysed. The peak value of the longitudinal displacement responses of the Pingsheng Bridge reaches 37.7 cm, exceeding the limited value of the bridge bearings and the expansion joints. Therefore, it should be necessarily controlled.

3. The viscous dampers, the friction pendulum bearings and the combined control strategy are investigated in vibration control. The reduction rates of the longitudinal displacement response achieved by viscous dampers, friction pendulum bearings, and the combined control with the optimized parameters are 34.54%, 28.22%, 42.17%, respectively, verifying the effectiveness of these control strategies for vibration mitigations of suspension bridges induced by vehicle braking forces. The combined control outperforms viscous dampers or friction pendulum bearings alone.

Acknowledgements

This work was supported by the grants (No. 51378504 and 51308549) from National Natural Science Foundation of China (NSFC), the project (No. IRT1287) from the department of education of China and the project (No. 13JJ7007) from Natural Science Foundation of Hunan Province, China. These supports are greatly appreciated.

References

Apaydin, N. M. 2010. Earthquake Performance Assessment and Retrofit Investigations of Two Suspension Bridges in Istanbul, *Soil Dynamics and Earthquake Engineering* 30(8): 702–710. http://dx.doi.org/10.1016/j.soildyn.2010.02.011

Ates, S.; Bayraktar, A.; Dumanoglu, A. A. 2006. The Effect of Spatially Varying Earthquake Ground Motions on The Stochastic Response of Bridges Isolated with Friction Pendulum Systems, *Soil Dynamics and Earthquake Engineering* 26(1): 31–44. http://dx.doi.org/10.1016/j.soildyn.2005.08.002

Cantero, D.; Gonzalez, A.; OBrien, E. J. 2011. Comparison of Bridge Dynamic Amplifications due to Articulated 5-axle Trucks and Large Cranes, *The Baltic Journal of Road and Bridge Engineering* 6(1): 39–47. http://dx.doi.org/10.3846/bjrbe.2011.06

Cheng, S. H.; Darivandi, N.; Ghrib, F. 2010. The Design of An Optimal Viscous Damper for A Bridge Stay Cable Using Energy-based Approach, *Journal of Sound and Vibration* 329(22): 4689–4704. http://dx.doi.org/10.1016/j.jsv.2010.05.027

Hart, G. C.; Jain, A.; Ekwueme, C. G. 2010. Smart Buildings: Viscous Dampers for A Tall Twisting Tower, *Structural Design of Tall and Special Buildings* 19(4): 373–396. http://dx.doi.org/10.1002/tal.608

Hoseini, S. M. S.; Fathi, M.; Vaziri, M. 2009. Controlling Longitudinal Safe Distance between Vehicles, *Promet-Traffic & Transportation* 21(5): 303–310. http://dx.doi.org/10.7307/ptt.v21i5.245

Hwang, J. S.; Wang, S. J.; Huang, Y. N.; Chen, J. F. 2007. A Seismic Retrofit Method by Connecting Viscous Dampers for Microelectronics Factories, *Earthquake Engineering and Structural Dynamics* 36(11): 1461–1480. http://dx.doi.org/10.1002/eqe.689

Hwang, J. S.; Tseng, Y. S. 2005. Design Formulations for Supplemental Viscous Dampers to Highway Bridges, *Earthquake Engineering and Structural Dynamics* 34(13): 1627–1642. http://dx.doi.org/10.1002/eqe.508

Jangid, R. S. 2008. Stochastic Response of Bridges Seismically Isolated by Friction Pendulum System, *Journal of Bridge Engineering* 13(4): 319–330. http://dx.doi.org/10.1061/(ASCE)1084-0702(2008)13:4(319)

Krishnamoorthy, A. 2011. Variable Curvature Pendulum Isolator and Viscous Fluid Damper for Seismic Isolation of Structures, *Journal of Vibration and Control* 17(12): 1779–1790. http://dx.doi.org/10.1177/1077546310384640

Liu, J.; Qu, W. L.; Pi, Y. L. 2010. Active/Robust Control of Longitudinal Vibration Response of Floating-Type Cable-Stayed Bridge Induced by Train Braking and Vertical Moving Loads, *Journal of Vibration and Control* 16(6): 801–825. http://dx.doi.org/10.1177/1077546309106527

Martinez-Rodrigo, M. D.; Lavado, J.; Museros, P. 2010. Dynamic Performance of Existing High-Speed Railway Bridges Under Resonant Conditions Retrofitted with Fluid Viscous Dampers, *Engineering Structures* 32(3): 808–828. http://dx.doi.org/10.1016/j.engstruct.2009.12.008

Panchal, V. R.; Jangid, R. S. 2009. Seismic Response of Structures with Variable Friction Pendulum System, *Journal of Earthquake Engineering* 13(2): 193–216. http://dx.doi.org/10.1080/13632460802597786

Peng, Y. H.; Wang, L. M. 2003. A Study on The Simulation of Vehicle's Braking Process, *Journal of Fuzhou University (Natural Science)* 31(2): 182–185 (in Chinese).

Qu, W. L.; Qin, S. Q.; Tu, J. W.; Liu, J.; Zhou, Q.; Cheng H.; Pi, Y. L. 2009. Intelligent Control for Braking-induced Longitudinal Vibration Responses of Floating-Type Railway Bridges, *Smart Materials and Structures* 18(12): 125003. http://dx.doi.org/10.1088/0964-1726/18/12/125003

Wang, X. Y.; Ni, Y. Q.; Ko, J. M.; Chen, Z. Q. 2005. Optimal Design of Viscous Dampers for Multi-Mode Vibration Control of Bridge Cables, *Engineering Structures* 27(5): 792–800. http://dx.doi.org/10.1016/j.engstruct.2004.12.013

Yang, M. G.; Li, C. Y.; Chen, Z. Q. 2013. A New Simple Non-linear Hysteretic Model for MR Damper and Verification of Seismic Response Reduction Experiment, *Engineering Structures* 52: 434–445. http://dx.doi.org/10.1016/j.engstruct.2013.03.006

Yang, M. G.; Chen, Z. Q.; Hua, X.G. 2011. An Experimental Study on Using MR Damper to Mitigate Longitudinal Seismic Response of A Suspension Bridge, *Soil Dynamics and Earthquake Engineering* 31(8): 1171–1181. http://dx.doi.org/10.1016/j.soildyn.2011.04.006

Yang, M. G.; Chen, Z. Q.; Hua, X. G. 2010. A New Two-Node Catenary Cable Element for The Geometrically Non-linear Analysis of Cable-Supported Structures, *Proceedings of the Institution of Mechanical Engineers, Part C: Journal of Mechanical Engineering Science* 224(C6): 1173–1183. http://dx.doi.org/10.1243/09544062JMES1816

Received 15 October 2012; accepted 2 November 2012